

The Benefits of Using Rubber Material in Two Variances: The Rubberized Concrete and the Natural Rubber Sheet, to Strengthen Concrete Barriers for Crash Energy Absorption



Lwin Lwin Aung^{ID}, Amphon Jarasjarungkiat^{*ID}

Department of Civil Engineering, School of Engineering, King Mongkut's Institute of Technology Ladkrabang, Bangkok 10520, Thailand

Corresponding Author Email: amphon.ja@kmitl.ac.th

Copyright: ©2024 The authors. This article is published by IETA and is licensed under the CC BY 4.0 license (<http://creativecommons.org/licenses/by/4.0/>).

<https://doi.org/10.18280/mmep.110808>

ABSTRACT

Received: 1 March 2024
Revised: 18 June 2024
Accepted: 28 June 2024
Available online: 28 August 2024

Keywords:

traffic road barrier, rubber material, finite element analysis, non-linear analysis, ABAQUS

Given the frequency of road accidents, a critical evaluation of the strength of road safety devices has become imperative. This research explores reinforced concrete barriers protected with rubber materials, incorporating different ratios of rubber powder derived from waste and various thicknesses of natural rubber sheets. Two approaches were employed: the first used crumb rubber from recycled tires to prepare barrier samples with varying rubber content ratios (0%, 15%, and 30% by volume); the second involved attaching concrete barriers with natural rubber sheets of different thicknesses (30 to 70mm). These barriers were subjected to frontal impact loads generated by vehicles traveling at 35mph. A crash dynamic was conducted using nonlinear explicit analysis in numerical modeling within a finite element simulation framework. The primary objectives were to monitor the crash energy absorbed by the rubber material, scrutinize deflection patterns, and assess overall energy absorption capabilities. The results indicated that natural rubber sheets absorbed approximately 20% to 47% of the maximum internal energy, reducing the impact on the concrete barrier. The 30% crumb rubber content of barriers also exhibited significantly higher energy dissipation than standard concrete barriers. This improvement in energy absorption and deflection properties carries significant implications, including reduced maintenance costs, decreased accident-related injuries, and minimized vehicle damage. These findings underscore the importance of developing and implementing rubber materials in two methods to enhance impact resistance and energy absorption in road safety infrastructure.

1. INTRODUCTION

Thailand's road fatality rates placed it among the top ten countries globally, with an estimated 33 deaths per 100,000 individuals in 2018. This, along with significant injuries and disabilities, emphasized the critical concern of road traffic accidents in Thailand. These accidents required multifaceted costs, including medical treatment, rehabilitation expenses, property damage, diminished quality of life, and the loss of human capital, collectively imposing a significant financial burden on the nation [1]. To reduce accidents, drivers must follow traffic rules, improve vehicle safety, install traffic devices on roads, and build and maintain high-quality roads. Among these devices, roadside barriers are essential for preventing fatalities and injuries by avoiding collisions with obstacles and protecting against lane-crossing accidents.

Road safety barriers come in various forms, such as steel, reinforced concrete, cables, and traffic barriers. Steel barriers dissipate energy from vehicles through the deformation of their structures, while reinforced concrete barriers absorb energy through friction. Researchers have investigated the strength of road safety barriers using various methods and materials. For instance, Dziewulski and Stanisławek [2]

studied the strength of road barriers by applying an impact load to barriers connected by a steel plate between two stamps, finding that better barrier deformation led to improved safety. Another study conducted by Radchenko [3] investigated the interaction of materials within the barrier with impact load, while Karunarathna et al. [4] introduced a simplified simulation technique that divides the barrier system into two sections: the Impact Zone and the Rigid Zone. This novel approach for concrete crash barriers used a validated numerical model to predict critical barrier performance parameters, providing insights not easily attainable through experimentation alone, such as internal energies and exit angles. A parametric study highlighted the importance of optimizing concrete material parameters to accurately simulate crash scenarios. The study demonstrated that increased impact speed presents greater risks to occupants compared to a more oblique impact angle.

Exploring the benefits of improved energy-absorbing concrete further showcased the model's capability to enhance road safety by analyzing and refining existing barrier designs. Comparisons between numerical simulations and experimental crash tests affirmed the reliability of the developed models for evaluating and advancing barrier

designs to bolster road safety. Mára et al. [5] used ultra-high-performance fiber-reinforced concrete with additional steel reinforcement bars to stop fast-moving vehicles. At the same time, Mohammed and Zain [6] created a new concrete barrier incorporating different ratios of polystyrene beads to enhance energy absorption. In their research on concrete barriers, Yin et al. [7] used the radial basis functions model to reduce computational optimization and simulation costs.

On the other hand, the growing global population has increased daily vehicle demand. In Thailand, 38 percent of the 250,000 metric tons of rubber products used in 2000 were allocated to vehicle tires. Consequently, the annual production of approximately 1.5 billion rubber tires had accumulated non-biodegradable waste, posing environmental hazards and consuming substantial space. Conventional disposal methods, such as burning waste tire rubber, contribute to toxic pollution, while landfilling exacerbates soil degradation. Researchers have explored recycling and repurposing waste tires for various applications to address these challenges [8-10]. This study aimed to uncover the benefits of incorporating recycled waste tires into concrete to create rubberized concrete barriers.

Several researchers have demonstrated that inputting rubber particles into concrete mixtures reduces the unit weight of the resulting rubberized concrete. Despite this weight reduction, rubberized concrete exhibited notable resilience compared to plain concrete, as evidenced by cube drop tests. However, this advantage comes with a trade-off, as increased rubber content tends to decrease compressive strength and increase energy dissipation. This unique behavior enhances the material's ability to withstand high-impact forces, making rubberized concrete a promising choice for applications requiring such resilience. In this study, the researcher investigated the performance of concrete barriers, including shredded waste tire chips (STC), as a partial replacement for coarse aggregate to improve impact energy absorption and reduce vehicle deceleration forces. Six concrete mix designs were prepared, with 0%, 20%, 40%, 60%, 80%, and 100% of the coarse aggregate replaced by STC. Static compression tests on cylindrical specimens (15cm×30cm) were conducted at 7 and 28 days to measure compressive strength and modulus of elasticity. Dynamic impact tests were performed on New Jersey-shaped concrete barriers using a 500kg bogie vehicle at 20kph to assess acceleration forces and energy absorption. Results showed that increasing STC content reduced compressive strength and modulus of elasticity, with maximum reductions of 65% and 63%, respectively. However, dynamic tests demonstrated significant improvements in impact performance, with barriers containing higher STC content absorbing more energy and generating lower peak acceleration forces. Optimal performance was observed in barriers with 20% to 40% STC replacement, balancing reduced concrete strength with enhanced impact energy absorption and reduced deceleration forces. This suggests their potential for safer and more effective roadside safety barriers [11]. The brittleness index of rubberized concrete showed an inverse relationship with the quantity of rubber particles, becoming less brittle and more ductile as rubber content increased. This transformation is attributed to the crack-arresting properties of the rubber particles, which absorb energy and allow for more plastic deformation and fewer fractures.

Elchalakani [12] investigated using rubberized concrete containing silica fumes, showing good performance and workability with rubber and concrete. The study used crumb

rubber from scrap tires and polypropylene fiber to enhance energy absorption [13]. An analysis of a mixture comprising 30% replacement of natural coarse aggregate, 5% crumb rubber, and 0.5 to 2% polypropylene fiber revealed that the combination of RCA and CR with 2% PP fiber content performed best. PP fibers enhance concrete's tensile capacity by creating strong bridges between aggregates, enabling the concrete to withstand additional loads even after reinforcement yields. Rubberized fiber-reinforced recycled aggregate concrete demonstrated higher energy absorption and deformation capacity, crucial for minimizing damage during traffic accidents. Including PP fibers and CR content, they significantly improved the deformation capacity of concrete beams. Low-reinforcement beams exhibited flexural failure, while high-reinforcement beams showed shear failure. Design equations for normal aggregate concrete tend to underestimate the capacity of low-reinforcement beams and overestimate high-reinforcement beams.

The F-shape design of the barrier was created to facilitate the gradual redirection of vehicles upon collision, preventing vehicles from rebounding into traffic or crossing into oncoming lanes. Concrete barriers are necessary for transportation safety by preventing vehicles from crossing the road. Studies on concrete containing crumb rubber showed that while mechanical properties like flexural strength, compressive strength, and modulus of elasticity decrease, impact resistance, ductility, flexibility, and energy absorption significantly improve. Impact resistance, defined as the ability of concrete to hold repeated impacts by absorbing energy without cracking or spalling, is crucial for concrete roadside barriers due to the high velocity of vehicle collisions. Including crumb rubber in concrete improves impact load behavior and fracture energy. For example, increased crumb rubber content results in 30% to 45% fracture energy enhancements for 5% to 20% rubber replacement levels, respectively.

Further research demonstrated that rubber particles in rubberized concrete enhance properties such as crack bridging, compression, twisting, and bending. These properties contribute to higher flexibility and energy absorption compared to conventional concrete. For instance, replacing natural sand with crumb rubber at 0% to 100% by volume showed a 160.8% increase in energy dissipation between the control and 100% rubber specimens. The toughness of rubber and its ability to absorb energy without fracturing under external loads also increases with higher rubber content. Therefore, including rubber particles in concrete increases toughness due to the material's bending properties, anti-cracking features, increased strain energy, and rubber particles' compressing and twisting abilities. Moreover, studies showed that adding CR improves concrete's ductility, reducing brittleness and leading to ductile failure rather than brittle failure. Thus, using waste tire rubber in concrete for road barriers presents a promising method for enhancing the safety and durability of these structures [14].

Additionally, the elastic modulus of rubberized concrete decreases with increasing rubber content. This reduction in modulus is linked to the heightened ductility of the material, enabling more deflection and deformation. Consequently, this reduces the forces experienced by structures and increases their capacity to absorb energy. The lower modulus of elasticity in rubberized concrete leads to greater deflection under load, potentially reducing the forces exerted on vehicles colliding with barriers made from this material. This aspect

proves promising for improving the safety of drivers and passengers in the unfortunate event of a collision.

The escalating environmental concerns associated with waste tire rubber disposal have spurred researchers to explore innovative solutions, including using rubber crumbs as a substitute for aggregates in concrete, known as rubberized concrete (RC). RC is recognized as an eco-friendly material that replaces a portion of its coarse aggregates with rubber aggregates. Extensive research has established that, as the rubber content in RC increases, the material demonstrates lower compressive strength but exhibits an increased capacity to absorb energy. This remarkable ability to absorb energy, particularly from impact loads, renders RC especially suited for applications like roadside barriers and blocks, where it plays an important role in minimizing the risk of driver and passenger injuries by decreasing the impact force.

Furthermore, the Thai government is searching to utilize surplus natural rubber production to benefit local farmers. This initiative aims to support rubber farmers while promoting a sustainable and cost-effective solution for transportation infrastructure. Research findings suggest that incorporating rubber sheets into concrete barriers enhances principal stress distribution and energy absorption, thereby reducing the impact of accidents. The study on the invention of natural rubber applied to concrete road barriers in Thailand found that these barriers significantly enhance road safety by absorbing impact forces, thereby reducing the severity of injuries, particularly head, skull, and neck injuries, for motorcyclists and other road users. The natural rubber fender barriers (NRFB) were shown to be economically viable, with cost analyses supporting their implementation. The barriers' design features, such as shear keys, were optimized to withstand high stress, and the results indicated a substantial potential for these barriers to lower accident-related costs. Future validation through laboratory tests adhering to EN1317 and NCHRP 350-Test Level 3 standards was recommended to confirm the findings. It was demonstrated that a 2-inch (50mm) rubber sheet absorbed 30% of the impact force. Moreover, the cost of covering a concrete barrier with a rubber sheet was lower than the cost incurred in an accident, highlighting the cost-effectiveness of using rubber materials in transportation infrastructure. According to Cheewapattananuwong and Chaloeuywares' study [15], covering a concrete barrier with a rubber sheet was approximately 2,311 Thai Baht per meter, whereas the cost of an accident was 3,360 Thai Baht per meter. The researchers based their model on the concrete barrier design recommended by the Road Design Department of Thailand. They conducted experiments to assess the benefits of integrating rubber materials into the barriers.

Thus, this paper explores the benefits of using rubber in transportation systems, increasing the strength of concrete barriers and reducing the costs of repairing concrete barriers. By incorporating these methodologies, the study aimed to highlight how rubber materials can enhance the performance of concrete barriers in terms of energy absorption and impact resistance. The first approach involved investigating the properties and performance of rubberized concrete, which includes crumb rubber, as opposed to standard concrete. This comparison aimed to show the potential improvements in flexibility, durability, and energy dissipation provided by rubberized concrete. The second approach evaluated the performance of concrete barriers augmented with rubber sheets. This method assessed how attaching rubber sheets could further improve the impact resistance and overall

effectiveness of concrete barriers in mitigating vehicle collision forces. By examining both methods, the research sought to provide comprehensive evidence supporting the integration of rubber materials into transportation infrastructure, ultimately aiming to enhance road safety and extend the lifespan of concrete barriers.

2. METHODOLOGY

2.1 Rubberized and normal concrete barriers

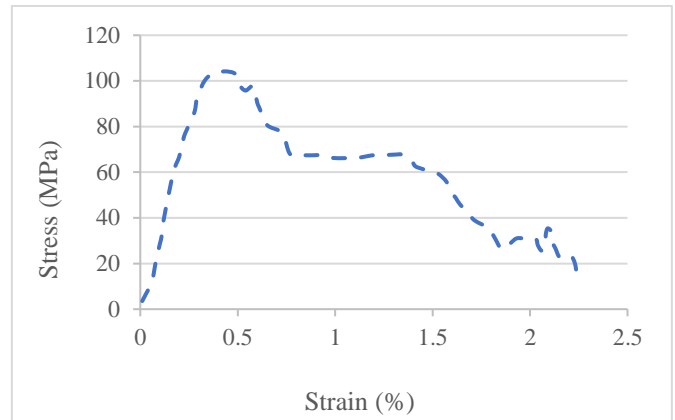
Pham et al. [16] meticulously prepared rubberized concrete (RC) specimens with varying rubber content (0%, 15%, and 30%). There were three sets of rubber crumbs such as 1-3mm, 3-5mm, and 5-10mm. The second set served as fine aggregate, while the last replaced the coarse aggregates. The varying rubber content (0%, 15%, and 30%) aimed to achieve static compressive strengths of 45MPa, 25MPa, and 15MPa. A water-soaking treatment was applied to enhance the mechanical properties of RC and bonding strength. Nine cylindrical specimens with a diameter of 100mm and a length of 200mm were prepared. A comprehensive analysis examined their compressive strength under both quasi-static and dynamic conditions. Dynamic tests were performed using a Split Hopkinson Pressure Bar (SHPB) to measure dynamic compressive strength under high strain rates. The study observed that higher rubber content in RC made the material more sensitive to strain rate, significantly enhancing its capacity to withstand high-impact forces at the cost of reduced compressive strength. The system comprised an incident bar (5500mm in length) and a transmitted bar (3000mm in length), both with a diameter of 100mm, constructed from stainless steel with specified properties: density of 7800kg/m³, Young's modulus of 240GPa, and elastic wave velocity of 5064m/s. A grease was applied at the interfaces between specimens and bars to minimize end friction confinement. A pulse shaper affixed to the impact end of the incident bar facilitated obtaining a half-sine stress waveform and extended the rising time of the incident pulse, thereby aiding in achieving stress equilibrium. Circular rubber pulse shapers, 3mm thick with a 20mm radius, were employed in all tests. A high-speed camera was utilized to document the failure progression of the specimens, allowing observation of dynamic properties such as failure progress, patterns, compressive strength, and energy absorption capacity. Tests were conducted on RC specimens with varying rubber contents at different pressures. Further analysis revealed that RC exhibited fewer brittle failure modes under high-impact loads than regular concrete. This unique behavior appeared to retard the development of cracks, contributing to the material's enhanced impact resistance.

Moreover, RC displayed significantly enhanced energy absorption capacity, especially under high strain rates, with the effect becoming more pronounced as rubber content increased. The study unequivocally demonstrated that RC was more sensitive to strain rate than conventional concrete. The dynamic increase factor (DIF) consistently exhibited a linear increase with higher rubber content, indicating higher values for rubberized concrete (RC) than conventional concrete. However, the study could not draw definitive conclusions regarding Young's modulus and axial strain behavior at peak load, as these parameters exhibited no distinct influence due to strain rate. These findings collectively underscore that RC could be remarkably effective in applications. They highlight the inherent trade-off between impact resistance and

compressive strength, underscoring RC's sensitivity to strain rate. These insights yield valuable data for engineering applications with critical material performance under high-rate loading. RC displayed exceptional impact resistance under high loading rates, remaining nearly intact even under identical impact conditions, while regular concrete fragmented into pieces. This underlines RC's significant potential for applications necessitating superior impact resistance. The study consistently highlighted RC's heightened sensitivity to strain rate, particularly with higher rubber content. This observation was pivotal in comprehending RC's behavior under high-rate loading scenarios. The study also systematically quantified and eliminated the influence of lateral inertia resistance from the experimental results. This meticulous approach allowed for a more precise assessment of the dynamic increase factor (DIF) specific to RC. The study's findings unequivocally illustrate that the absorbed energy, when normalized by RC's compressive strength, surpasses that of regular concrete, conclusively illustrating RC's heightened energy absorption capacity. The study highlighted a significant enhancement in energy absorption for rubberized concrete (RC) specimens, particularly those with different rubber content, under impact loading conditions. Comprehensive studies are imperative to understand rubberized concrete's (RC) mechanical properties under dynamic loading conditions, such as compressive strength, strain, energy absorption, and modulus. These studies should encompass multifaceted factors influencing material behavior, including the strain rate, inertial effect, viscosity effect, and the role of coarse aggregate properties.

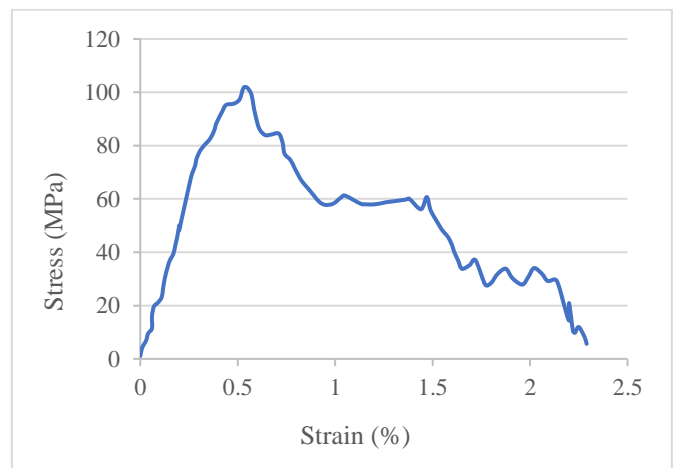
The study conducted by Pham et al. [16] focused on investigating the dynamic compressive strength by analyzing stress-strain curves of various rubberized concrete models at different strain rates. Among the specimens with varying rubber content (0%, 15%, and 30%) at a strain rate of 103 s⁻¹, the 15% rubberized concrete exhibited failure from the edges, with the middle part remaining intact. The 30% rubberized concrete only showed small cracks on the circumference, maintaining its cylindrical shape with fewer fragments. 125s⁻¹, normal concrete shattered into smaller pieces, while the 15% rubberized concrete broke into a few large pieces. The 30% rubberized concrete outperformed both, with only slight damage to the outer edge. Even at 151s⁻¹, 30% of rubberized concrete had cracks near the circumference but remained intact in the middle. This demonstrated that the impact load damage to rubberized concrete decreased with higher rubber content, especially with 30% rubber content. In Figure 1, the stress-strain curves of normal concrete at 116s⁻¹ and 140s⁻¹ strain rates showed that it shattered into smaller pieces.

On the other hand, in Figure 2 and Figure 3, the stress-strain curves of 15% and 30% rubberized concrete at various strain rates around 100s⁻¹ demonstrated failure from the edges up to over 180s⁻¹, where it shattered into smaller pieces. The effect of increased strain rate on the failure mode of concrete varies significantly between normal concrete and rubberized concrete. While normal concrete exhibits considerable changes in failure mode under varying strain rates, rubberized concrete demonstrates greater resilience. The superior performance of rubberized concrete can be attributed to the crack-arresting characteristic of rubber aggregates, as mentioned in a previous study, and the bridging effect of coarse rubber aggregates between cracks, reducing crack intensity. This suggested that rubberized concrete was highly appropriate for structures subjected to impact or blast loadings.



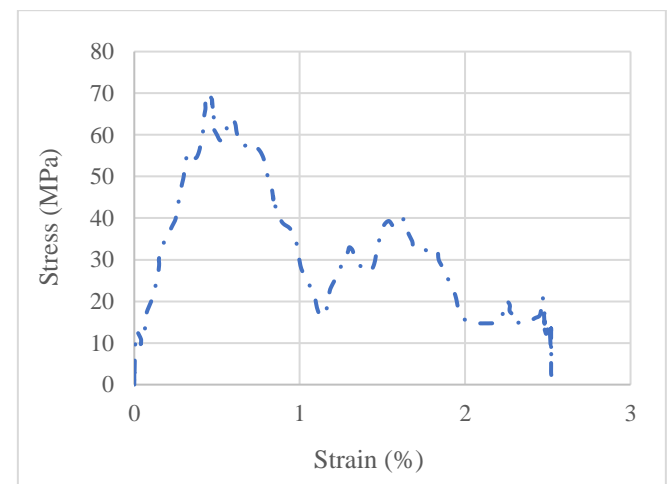
Note: Reproduced from the study conducted by Pham et al. [16]

Figure 1. Stress-strain curves of NC



Note: Reproduced from the study conducted by Pham et al. [16]

Figure 2. Stress-strain curves of RC 15%



Note: Reproduced from the study conducted by Pham et al. [16]

Figure 3. Stress-strain curves of RC 30%

Table 1. Material properties of normal concrete (NC) and rubberized concrete barriers (RC)

Material	Density (kg/m ³)	Modulus of Elasticity (GPa)
Steel	7850	210
NC	2350	28.4
RC (15%)	2091	24.8
RC (30%)	1833	15.99

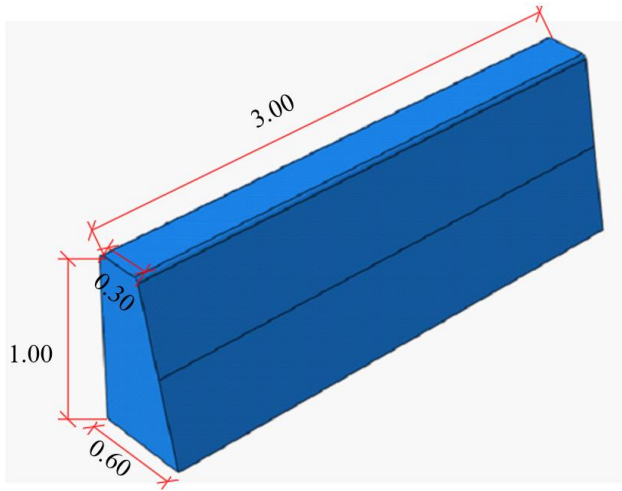


Figure 4. Design of reinforced concrete barrier for both NC and RC

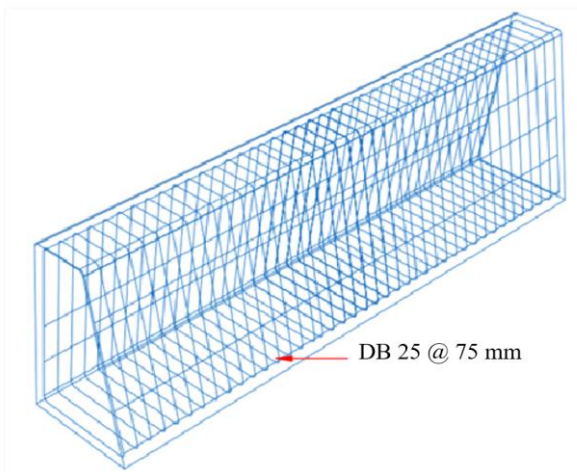


Figure 5. Arrangement of reinforced steel bars and stirrups in the barrier

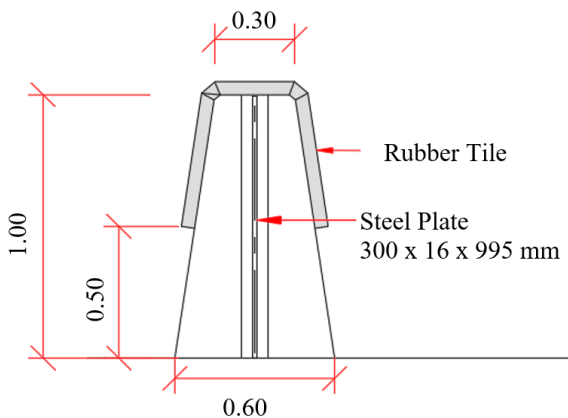


Figure 6. The model design from the rural department of Thailand

First, a concrete barrier of 3m in length, 1m in height, and 0.6m in width was made, as shown in Figure 4. Then, 25mm-diameter reinforced steel bars and stirrups were embedded at 75mm spacing within the concrete barrier, as described in Figure 5. The steel density and modulus of elasticity were 7850kg/m³ and 210GPa. The normal concrete barrier (NC-0% RC) density was 2350kg/m³, while the densities for RC 15%

and 30% were 2091kg/m³ and 1833kg/m³, respectively. The moduli of elasticity for these variants were 28.4GPa for NC, 24.8GPa for RC 15%, and 15.99GPa for RC 30%, as reported in the research [16]. Stress-strain data from a strain rate of 116s⁻¹ indicating failure were applied to the normal concrete barrier (NC). In contrast, the data for rubberized concrete RC 15% and RC 30% were derived from strain rates of 165s⁻¹ and 182s⁻¹, respectively-the parameters for density and modulus of elasticity for all models detailed in Table 1.

2.2 Reinforced concrete barrier with natural rubber sheet

Hyperelastic behavior is important in modeling the rubber sheet used in the reinforced concrete barrier. Many hyperelastic models are available, and each model has strengths and limitations. Haines and Wilson's model is a high-order Rivlin series, meaning it is a polynomial function with high accuracy. The Arruda-Boyce model is a higher-order model with a statistical approach to material behavior. The Ogden model is a higher-order hyperelastic form that has been shown to have high accuracy for predicting buckling and calculating displacements.

On the other hand, low-order models such as Neo-Hookean are simpler but may not accurately capture material behavior at large deformations. Mooney-Rivlin is a well-known low-order model often used due to its simplicity and good agreement with moderate deformations. The Mooney-Rivlin model allows for characterizing a wide range of hyperelastic materials, including both isotropic and anisotropic behaviors.

Its formulation can accommodate various material properties and responses, making it suitable for modeling materials such as rubber, elastomers, and soft tissues. Compared to simpler models, this model offers a more accurate representation of the stress-strain behavior of hyperelastic materials. It can capture nonlinear stress-strain responses, including large deformations and complex material behavior under different loading conditions. The Mooney-Rivlin model has been extensively validated against experimental data for various materials and loading conditions. Its widespread use and validation across different industries and applications contribute to its credibility and reliability in predicting material behavior. While the Mooney-Rivlin model requires more parameters than simpler models, these additional parameters provide greater flexibility in accurately capturing the material's behavior under different loading conditions. With careful parameter calibration based on experimental data, the model can provide highly accurate predictions of material response [17-19]. The Mooney-Rivlin hyperelastic model was chosen for the rubber sheet material in this study due to its simple order and good agreement in predicting deformations.

Mooney-Rivlin hyperelastic form:

$$U=C_{10}(\bar{I}_1-3)+C_{01}(\bar{I}_2-3)+1/D_1(J^e-1)^2 \quad (1)$$

$$\bar{I}_1 = J^{(-\frac{2}{3})}(\lambda_1^2 + \lambda_2^2 + \lambda_3^2) \quad (2)$$

$$\bar{I}_2 = J^{(-\frac{4}{3})}(\lambda_1^2\lambda_2^2 + \lambda_2^2\lambda_3^2 + \lambda_3^2\lambda_1^2) \quad (3)$$

where, U is the reference volume's strain energy, C₁₀, C₀₁, and D₁ are material parameters of temperature-dependent, strain invariants of first and second deviatoric are \bar{I}_1 and \bar{I}_2 , a ratio of the total volume is J, and last one λ is principal stretches. The

researchers tested the energy absorption of rubber sheets of various thicknesses (ranging from 30mm to 70mm) when attached to a normal concrete reinforced barrier that was 3 meters in length and 0.5 meters in height. The researchers used data 0.79 and 0.101 from previous tests [19] to determine the values of C_{10} and C_{01} and then modeled the normal concrete barrier with the attached rubber sheet. This study considered the concrete barrier design outlined in Figure 6 by the Rural Department of Thailand, as depicted in Figure 7. This experiment aimed to investigate how much energy the rubber sheet could absorb under different conditions.

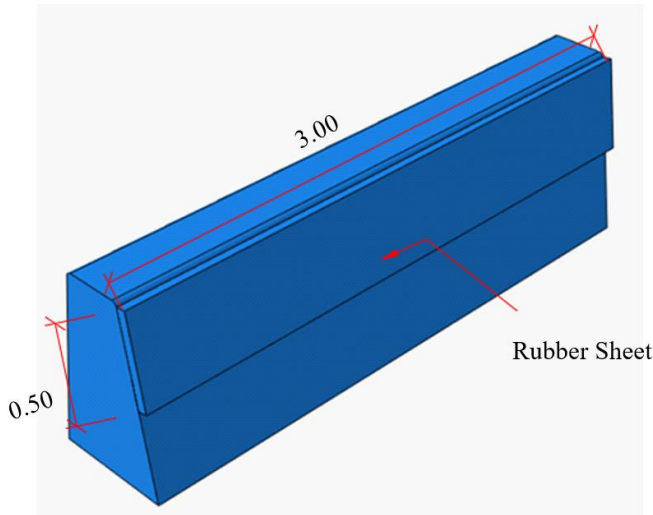


Figure 7. Model of reinforced NC barrier with rubber sheet

2.3 Meshing

In this study, finite element analysis (FEA) utilized various mesh element shapes to ensure accurate results, including hexahedral, hexahedral-dominated, tetrahedral, and wedge forms. Hexahedral elements were predominantly chosen for their favorable convergence rate and accuracy performance. Mesh sensitivity analysis is critical in computational studies because it evaluates how changes in mesh parameters impact numerical results, thereby ensuring the accuracy and reliability of simulations. Researchers systematically adjust parameters such as element size or density and observe corresponding changes in outcomes such as solution convergence, gradients, or boundary conditions to determine the optimal mesh configuration. This process validates the numerical model and enhances confidence in its predictive capabilities, making findings suitable for publication in academic journals. Mesh sensitivity analysis in this research was conducted to validate the robustness of numerical simulations across varying discretization levels, as depicted in Figure 8. This practice underscores the credibility of computational studies by demonstrating the model's ability to produce reliable results under different mesh configurations, thereby supporting reproducibility and advancing scientific understanding in the field.

In the study, an 8-node linear brick element type was chosen for modeling the normal concrete barrier (NC) and the rubberized concrete barrier (RC), resulting in 12,840 elements and 308,160 degrees of freedom for these components. Specifically, the rubber sheets alone utilized 600 elements and 14,400 degrees of freedom. A 2-node linear truss element type was employed for the reinforced steel elements, resulting in

590 elements and 3,540 degrees of freedom. Stirrups were modeled using 2,301 elements and 13,806 degrees of freedom. These details are summarized in Table 2. The distribution of degrees of freedom for solid and truss elements is illustrated in Figure 9. Visual representations of the mesh shapes and structures for each model were provided in Figure 10 and Figure 11, offering a clear illustration of the finite element mesh utilized in the analysis. This meticulous approach to meshing significantly contributed to the accuracy and reliability of the finite element simulation results.

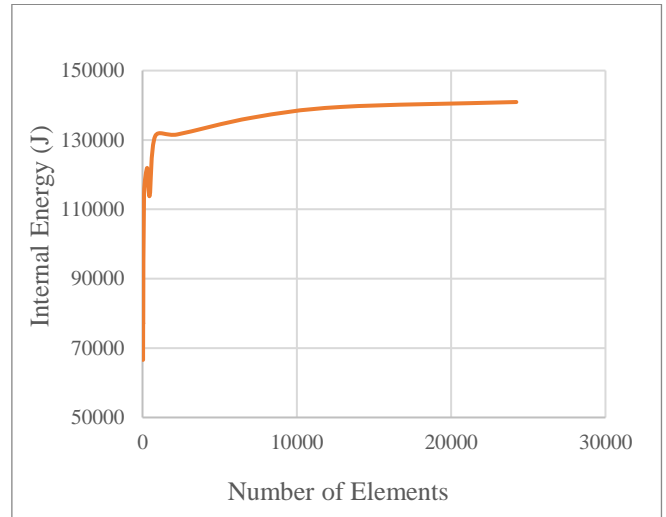


Figure 8. Mesh sensitivity testing

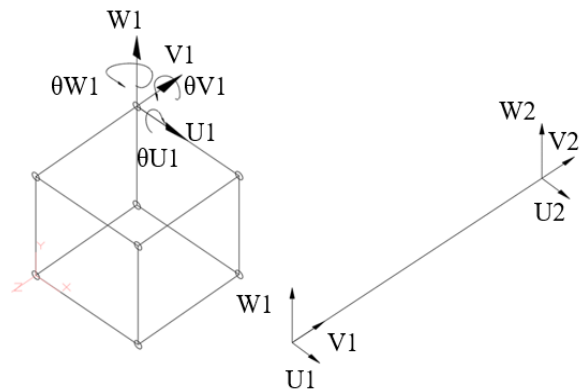


Figure 9. Degree of freedoms for solid and truss elements

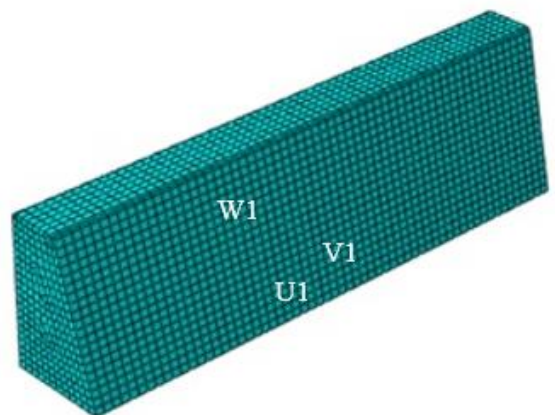


Figure 10. Meshing of NC and RC barriers

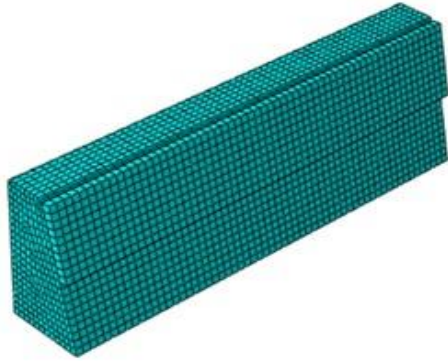


Figure 11. Meshing of RS after assembling each material

Table 2. Elements and degree of freedoms

Material	Elements	Degree of Freedoms
Barrier	12,840	308,160
Rubber sheet	600	14,400
Steel bars	590	3,540
Stirrups	2,301	13,806

2.4 Analysis with finite element method

Finite element analysis (FEA) stands out as an affordable and widely used method for simulating the behavior of structures under different loading and boundary conditions. This computational technique provides stress and strain distributions, deformation patterns, and failure modes within a structure without physical testing. The process involves dividing a complex structure into discrete elements, solving the governing equations for these elements under various loads, and gaining insights into the overall behavior of the structure.

FEA is applicable across a wide range of structural complexities, from simple beams to intricate three-dimensional structures. With a robust understanding of rubberized concrete properties, researchers can harness FEA to model and investigate the behavior of barriers under diverse impact scenarios. This enables a comprehensive assessment of barrier performance, particularly regarding internal energy absorption and deflection characteristics.

The authors employed numerical simulation with the finite element method, ABAQUS [20] to conduct frontal crash tests on three types of models: normal concrete (NC), rubberized concrete (RC), and reinforced concrete with a rubber sheet (RS). This methodology was chosen due to the expense and time constraints associated with physical experimental tests, while numerical simulations offer rapid and efficient results. The finite element method was valuable for investigating intricate mechanical and structural behaviors within a controlled and adaptable environment. In static analysis, the model is considered to be at rest, and the effects of inertia are neglected. This method is suitable for analyzing structures under constant or slowly varying loads, where the structure's response time is much longer than the loading time.

Dynamic analysis, in contrast, considers the effect of inertia and is well-suited for analyzing structures subjected to sudden and rapidly varying loads, such as impact and blast loads. In dynamic analysis, two main methods are employed: implicit and explicit. The implicit method is more accurate and has no mathematical time limit for the solution, whereas the explicit method is efficient for large models with short analysis times. This study chose the explicit analysis method due to its

suitability for dynamic problems with short analysis times and its efficiency in handling large models with small increments. Moreover, explicit analysis does not require the formation of tangent stiffness matrices, which can save computational time and resources. Consequently, dynamic analysis was applied to the models in this study to explore the characteristics of the barriers.

The formula of the dynamic explicit method:

$$\dot{u}_{(i+1/2)}^N = \dot{u}_{(i-1/2)}^N + \left[(\Delta t_{(i+1)} + \Delta t_{(i)}) / 2 \right] \cdot \ddot{u}_{(i)}^N \quad (4)$$

$$u_{(i+1)}^N = u_{(i)}^N + \Delta t_{(i+1)} \dot{u}_{(i+1/2)}^N \quad (5)$$

$$\ddot{u}_{(i)}^N = (M^{NJ})^{-1} (P_{(i)}^J - I_{(i)}^J) \quad (6)$$

Hence, u^N is the degree of freedom, i is the increment number in step, \dot{u}^N is velocity, \ddot{u}^N is acceleration. M is the mass matrix, P is applied load vector, and IJ internal force vectors are necessary for this method. The step time varied from 0.18 to 0.022 according to models.

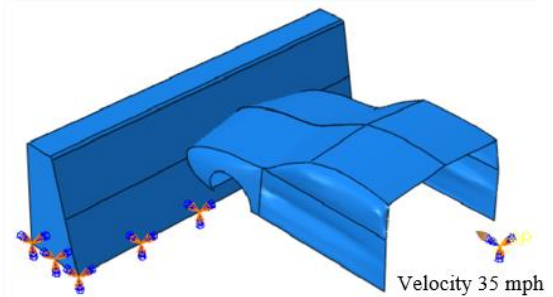


Figure 12. Position of a vehicle from NC and RC barriers

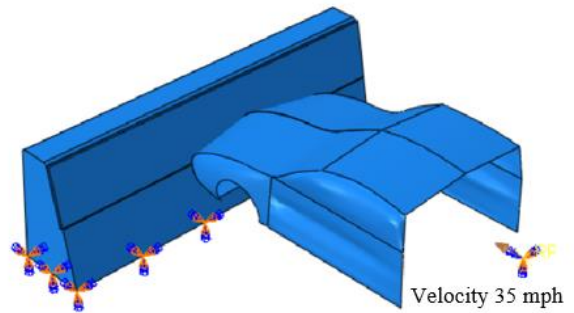


Figure 13. Position of vehicles from RS

In this study, our focus extended beyond merely determining the maximum deflection of barriers. We deliberately narrowed our scope to maintain control over the analysis by excluding numerous variations. Specifically, we concentrated on fixing degrees of freedom from the bottom surfaces of barriers in normal concrete (NC), rubberized concrete (RC), and barriers integrated with rubber sheets. The assembled passenger vehicle weighed 1240kg, and the barriers were depicted in Figure 12 and Figure 13, respectively. In this study, the vehicle was considered a rigid body. Subsequently, a velocity of 35mph, sourced from the National Highway Traffic Safety Administration, was applied to the barriers to simulate a frontal impact. Frontal impacts are deemed one of the most severe collisions due to the high energy and forces involved. Therefore, in this study, the vehicle was positioned

at a 90-degree angle to simulate a frontal impact load. Subsequently, the internal energy of the concrete and rubber materials was analyzed.

3. RESULTS AND DISCUSSION

3.1 Comparisons of NC and RC (15% and 30%)

The maximum internal energy recorded for the 15 percent and 30 percent rubberized concrete (RC) barriers stood at 140 and 141kJ, respectively. In contrast, the internal energy for the normal concrete (NC) barrier was 139kJ following contact with the vehicle before returning to its original state. Figure 14 presents a graphical comparison between the normal concrete barrier (NC) and rubberized concrete (RC), with a more detailed view provided in Figure 15. The findings underscored the superior impact resistance and higher compressive strength of the rubberized concrete barrier (RC), resulting in a deceleration of crack propagation, as highlighted in the above topic [15]. While the disparity in internal energy between the 15 percent and 30 percent rubberized concrete barriers was not substantial-indicating that increasing the rubber content did not lead to a significant boost in energy absorption-the discernible difference lay in displacement. The 15 percent and 30 percent rubberized concrete barriers exhibited displacements of 23.8mm and 31mm, respectively, compared to 23.2mm for the normal concrete barrier. This suggested that the rubberized concrete barriers could withstand more deflection after accidents. Further details of the results for energy absorption and displacement were provided in Table 3.

3.2 Comparisons of NC and RS (30-70mm)

The assessment of concrete barriers, incorporating rubber sheets with thicknesses ranging from 30 to 70mm under the same distance and load conditions as the prior testing, revealed the energy-absorbing capacity of the rubber sheets in safeguarding the concrete barrier. The internal energy of the rubber sheets exhibited a gradual increase from 18 to 64kJ with the augmentation of rubber thickness. Notably, the internal energy of the concrete in models with rubber sheets (RS) surpassed that of normal concrete, ranging from 116kJ to 75kJ. Figure 16 illustrates the peak internal energy, with NC registering 139kJ. In contrast, the concrete barrier with rubber sheets (RS 30-70mm) exhibited a trend from 116kJ to 74kJ, providing a more detailed view in Figure 17.

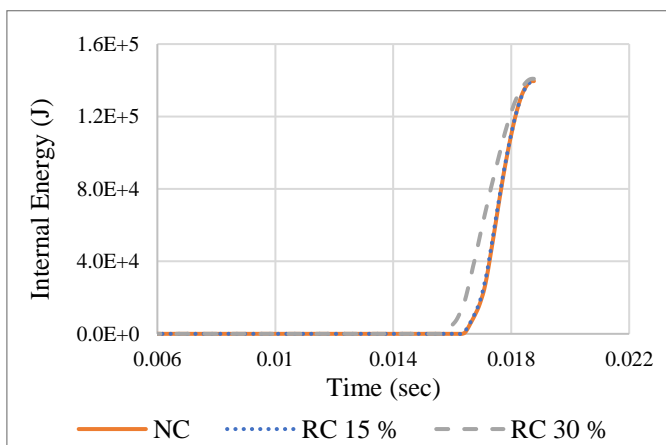


Figure 14. Internal energy of concrete barriers for NC, RC 15% and RC 30%

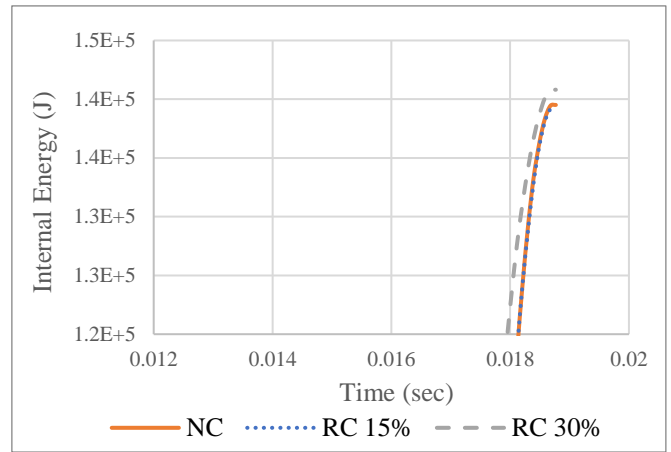


Figure 15. Zoom in the values of Figure 14

Table 3. Maximum internal energy and displacement of concrete at a peak point

Types of Barriers	Maximum Internal Energy (kJ)	Displacement (mm)
NC	139	23.2
RC (15%)	140	23.8
RC (30%)	141	31.0

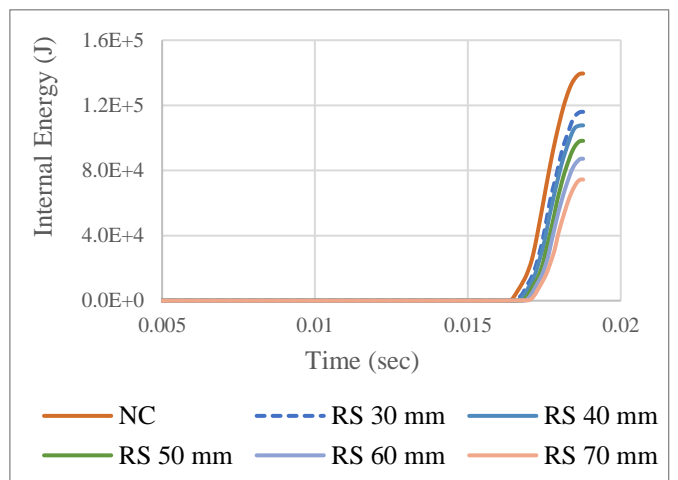


Figure 16. Internal energy of concrete barriers for NC and RS (30-70mm)

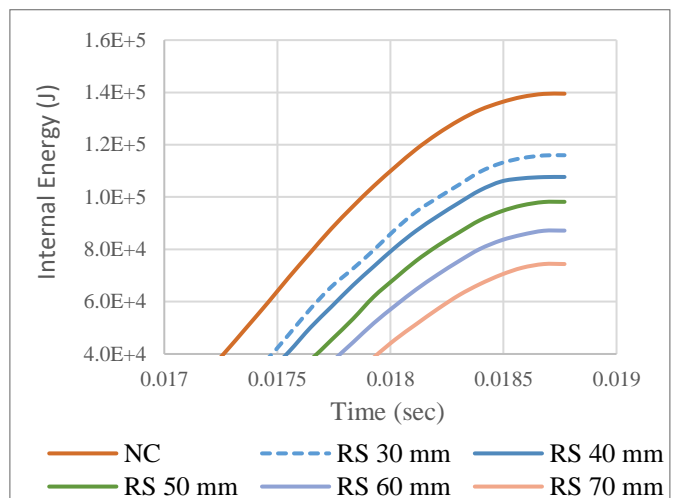


Figure 17. Zoom in the values of Figure 16

Table 4. Maximum internal energy and displacement of concrete and rubber sheets at a peak point

Types of Barriers	Maximum Internal Energy of Concrete (kJ)	Maximum Internal Energy of Rubber (kJ)	Displacement (mm)
NC	139	-	23.2
RS (30mm)	116	18	22.0
RS (40mm)	108	27	21.0
RS (50mm)	98	37	19.8
RS (60mm)	87	49	18.5
RS (70mm)	74	64	17.0

Furthermore, the displacements observed in concrete barriers with varying thicknesses of rubber sheets were lower than those in the normal concrete barrier. Specifically, the displacement for NC was 23.2mm, whereas for various rubber sheet configurations, it ranged from 22 to 17mm, as outlined in Table 4. Incorporating an absorbable rubber sheet demonstrated the potential to shield the concrete from damage by nearly 17 to 47 percent. Consequently, the utilization of rubber sheets emerged as an effective strategy to absorb internal energy and mitigate the extent of damage to concrete barriers.

4. CONCLUSIONS

The following effects were found after applying nonlinear dynamic tests with rubber material:

(1). Nonlinear explicit analysis using the ABAQUS simulation framework validated the enhanced performance of barriers incorporating rubber materials under impact loads. This comprehensive numerical modeling provided valuable insights into crash dynamics and the benefits of rubber materials in barrier design.

(2). The addition of rubber particles to concrete reduces the density of the material because rubber has a lower density than concrete. This also decreases the modulus of elasticity, describing the material's ability to resist deformation under stress. Consequently, the compressive strength of rubberized concrete is typically lower than that of conventional concrete. However, this reduction can benefit applications such as crash barriers, where energy absorption and reduced impact severity are desired. Rubberized concrete can withstand greater deflections, and incorporating crumb rubber from recycled tires into concrete barriers significantly improves energy absorption. Barriers with 30% crumb rubber content exhibited up to a 47% improvement in internal energy absorption compared to standard concrete barriers.

(3). Several models exist for hyperelastic materials, including Mooney-Rivlin, Neo-Hookean, Ogden, and Yeoh. Among these, the Mooney-Rivlin model is well known for its simplicity and effectiveness in predicting deformations.

(4). The study aimed to evaluate the effectiveness of reinforced concrete barriers with a rubber sheet in reducing the severity of impact forces compared to reinforced concrete barriers. The rubber sheet was attached to the reinforced concrete barrier to absorb the impact energy of colliding vehicles. The results showed that the reinforced concrete barrier with a rubber sheet could absorb the energy and reduce impact forces than the normal concrete barriers. This was attributed to the high elasticity and deformability of the rubber material, which allowed it to absorb and dissipate energy

during collisions. Attaching natural rubber sheets of various thicknesses (30 to 70mm) to concrete barriers increased their impact resistance. The study found that barriers with natural rubber sheets absorbed crash energy more efficiently, resulting in better deflection patterns and reduced structural damage. Additionally, the study indicated that covering a barrier with a rubber sheet was more cost-effective than repairing a damaged barrier after an accident. Using rubber materials in reinforced concrete barriers offers several advantages, including improved energy absorption and reduced costs. This can be especially beneficial in countries like Thailand, where natural rubber is overproduced, providing a new use for the material.

(5). The displacements observed in the models indicated a clear correlation between rubber content and displacement reduction. Barriers with 30% crumb rubber content showed reduced displacements compared to standard concrete barriers, demonstrating better impact resistance and structural integrity. Similarly, barriers with natural rubber sheets found lower displacements, with the 70mm thick sheets providing the most significant reduction. This reduction in displacement proves the effectiveness of rubberized materials in increasing the overall performance of concrete barriers under impact loads.

(6). Using crumb rubber powder in concrete mixtures can help reduce the environmental impact of waste tire disposal while upgrading the performance of roadside safety barriers. Additionally, using recycled rubber materials in construction can economically reduce the demand for natural materials and manufacturers.

Therefore, this study aims to investigate the energy absorption of concrete barriers using nonlinear finite element analysis by instructing models with rubber materials from different perspectives. Increasing the energy absorption of concrete barriers can reduce maintenance costs, injuries from accidents, and vehicle damage. The many benefits of using rubber materials in traffic devices are evident.

Extensive research is required to study rubber sheets using higher-order forms of the Ogden model to account for large displacements observed with natural rubber. Comprehensive experimental crash tests are also necessary to evaluate the performance of barriers incorporating rubber materials.

REFERENCES

- [1] Chantith, C., Permpoonwivat, C.K., Hamaide, B. (2021). Measure of productivity loss due to road traffic accidents in Thailand. *IATSS Research*, 45(1): 131-136. <https://doi.org/10.1016/j.iatssr.2020.07.001>
- [2] Dziejwulski, P., Stanisławek, S. (2019). The impact of forming processes on road barrier strength. In *Proceedings of the 15th Conference on Computational Technologies in Engineering*, Jora Wielka, Poland, p. 020003. <http://doi.org/10.1063/1.5092006>
- [3] Radchenko, A. (2017). Numerical simulation of the reinforced concrete barrier destruction at impact. *Aeronautics and Aerospace Open Access Journal*, 1(3): 103-106. <https://doi.org/10.15406/aaaj.2017.01.00013>
- [4] Karunaratna, S., Linforth, S., Kashani, A., Liu, X., Ngo, T. (2024). Numerical investigation on the behaviour of concrete barriers subjected to vehicle impacts using modified K&C material model. *Engineering Structures*, 308: 117943. <https://doi.org/10.1016/j.engstruct.2024.117943>
- [5] Mára, M., Konrád, P., Fornůšek, J., Zatloukal, J.,

- Frydrýn, M., Nouzovský, L., Mičunek, T., Sovják, R. (2020). Development of mobile road barrier made of ultra-high-performance fibre-reinforced concrete. *Materials Today: Proceedings*, 32: 162-167. <https://doi.org/10.1016/j.matpr.2020.04.182>
- [6] Mohammed, H.J., Zain, M.F.M. (2016). Experimental application of EPS concrete in the new prototype design of the concrete barrier. *Construction and Building Materials*, 124: 312-342. <https://doi.org/10.1016/j.conbuildmat.2016.07.105>
- [7] Yin, H., Fang, H., Wang, Q., Wen, G. (2016). Design optimization of a MASH TL-3 concrete barrier using RBF-based metamodels and nonlinear finite element simulations. *Engineering Structures*, 114: 122-134. <https://doi.org/10.1016/j.engstruct.2016.02.009>
- [8] Jafari, K., Toufigh, V. (2017). Experimental and analytical evaluation of rubberized polymer concrete. *Construction and Building Materials*, 155: 495-510. <https://doi.org/10.1016/j.conbuildmat.2017.08.097>
- [9] Elchalakani, M., Aly, T., Abu-Aisheh, E. (2016). Mechanical properties of rubberised concrete for road side barriers. *Australian Journal of Civil Engineering*, 14(1): 1-12. <http://doi.org/10.1080/14488353.2015.1092631>
- [10] Siddika, A., Al Mamun, M.A., Alyousef, R., Amran, Y.M., Aslani, F., Alabduljabbar, H. (2019). Properties and utilizations of waste tire rubber in concrete: A review. *Construction and Building Materials*, 224: 711-731. <https://doi.org/10.1016/j.conbuildmat.2019.07.108>
- [11] Atahan, A.O., Sevim, U.K. (2008). Testing and comparison of concrete barriers containing shredded waste tire chips. *Materials Letters*, 62(21-22): 3754-3757. <https://doi.org/10.1016/j.matlet.2008.04.068>
- [12] Elchalakani, M. (2015). High strength rubberized concrete containing silica fume for the construction of sustainable road side barriers. In *Structures*. Elsevier, 1: 20-38. <https://doi.org/10.1016/j.istruc.2014.06.001>
- [13] Shahjalal, M., Islam, K., Ahmed, K.S., Tamanna, K., Alam, M.S. (2020). Mechanical characterization of rubberized fiber reinforced recycled aggregate concrete for bridge barriers. In *IABSE-JSCE Joint Conference on Advances in Bridge Engineering-IV*, Dhaka, Bangladesh, pp. 978-984.
- [14] Sheraz, M., Yuan, Q., Alam, M., Javed, M.F., Rehman, M.F., Mohamed, A. (2023). Fresh and hardened properties of waste rubber tires based concrete: A state art of review. *SN Applied Sciences*, 5(4): 119. <https://doi.org/10.1007/s42452-023-05336-5>
- [15] Cheewapattananuwong, W., Chaloeypware, P. (2020). The innovation of natural rubber applied with concrete road barriers in Thailand. *Advances in Science and Technology*, 103: 55-61. <https://doi.org/10.4028/www.scientific.net/AST.103.55>
- [16] Pham, T.M., Chen, W., Khan, A.M., Hao, H., Elchalakani, M., Tran, T.M. (2020). Dynamic compressive properties of lightweight rubberized concrete. *Construction and Building Materials*, 238: 117705. <https://doi.org/10.1016/j.conbuildmat.2019.117705>
- [17] Khajehsaeid, H., Arghavani, J., Naghdabadi, R. (2013). A hyperelastic constitutive model for rubber-like materials. *European Journal of Mechanics-A/Solids*, 38: 144-151. <https://doi.org/10.1016/j.euromechsol.2012.09.010>
- [18] Szurgott, P., Jarzębski, Ł. (2019). Selection of a hyperelastic material model-a case study for a polyurethane component. *Latin American Journal of Solids and Structures*, 16: e191. <https://doi.org/10.1590/1679-78255477>
- [19] Saidou, A., Gauron, O., Busson, A., Paultre, P. (2021). High-order finite element model of bridge rubber bearings for the prediction of buckling and shear failure. *Engineering Structures*, 240: 112314. <https://doi.org/10.1016/j.engstruct.2021.112314>
- [20] ABAQUS Analysis User's Manual. Simulia Abaqus FEA software. <https://classes.engineering.wustl.edu/2009/spring/mase5513/abaqus/docs/v6.6/books/usb/default.htm>, accessed on Aug. 6th, 2024.